Research on Fault Diagnosis Algorithm of Air Compressor Based on Low-Rank Matrix Recovery

Tianming Yu, Cheng Long, Guoliang Feng,

***Abstract*—Air compressors are crucial in industrial production, but issues such as equipment aging and improper operation can lead to faults, severely impacting efficiency and safety. Traditional MFCC spectrogram-based diagnostic methods are challenged by background noise interference, making accurate fault feature extraction difficult. To address this, this study proposes an air compressor fault identification algorithm based on low-rank matrix recovery. By applying low-rank background modeling to the MFCC spectrogram to eliminate background noise, the algorithm effectively extracts primary features. The MobileNetV2 model is then used to extract features from the MFCC foreground images, followed by dimensionality reduction using Principal Component Analysis (PCA). The reduced-dimensional fault features are analyzed using k-means clustering. Experimental results show that for Data 2, the VGG19 model achieved an accuracy of 95.90%, an F1-score of 0.91, and a recall of 0.93, with a processing time of 1916 seconds. In comparison, the ResNet50 model attained an accuracy of 94.88%, an F1-score of 0.91, and a recall of 0.93, with a processing time of 826 seconds. These results demonstrate that the foreground features obtained through low-rank background modeling exhibit superior performance in fault identification and clustering, enhancing the accuracy and stability of fault diagnosis. Thus, the proposed algorithm shows promising potential for diagnosing and repairing air compressor faults.**

***Index Terms*—MFCC, Low-rank Background Modeling, K-means, Fault Recognition.**

I. Introduction

THE operational state of an air compressor holds paramount importance in industrial production. However, as the service life of air compressors extends, various factors such as improper operation, inadequate equipment maintenance, and aging equipment can lead to frequent failures. These failures not only diminish production efficiency but also elevate safety risks, thereby compromising the quality and safety standards of industrial production. Consequently, the accurate diagnosis of air compressor faults and the implementation of suitable maintenance measures are crucial for enhancing efficiency and safety levels in industrial production[1].

In recent years, deep learning has emerged as a prominent area of research across various domains, notably in image recognition [2] and speech processing [3]. With increasing interest, scholars have begun exploring its application in mechanical equipment fault diagnosis [4],[5], thereby advancing fault diagnosis technology in this domain. A crucial aspect of utilizing sound signals for air compressor fault diagnosis lies in effective feature extraction, which involves isolating valuable information from sound signals while eliminating interference. Commonly employed methods for sound feature extraction include Linear Predictive Cepstrum Coefficient (LPCC) [6], Mel Frequency Cepstrum Coefficient (MFCC) [7], and Gamma Pass Frequency Cepstrum Coefficient (GFCC) [8]. In the realm of signal feature training and recognition, prevalent intelligent algorithms include artificial neural networks (ANN) [9], hidden Markov models (HMM) [10], and support vector machines (SVM) [11]. Noteworthy among existing diagnostic methods based on acoustic signals, Hoang et al. [12] utilized a diagnostic model employing adaptive noise cancellation and deep learning for bearing fault diagnosis. Janssen et al. [13] first transformed time-domain signals of bearings and gears in gearboxes into frequency-domain signals, employing convolutional neural networks for fault diagnosis, demonstrating practical utility in experimental settings. Kong Xiaojia, Su Yuanhao, and others [14] proposed a composite gearbox fault diagnosis method based on a deep adversarial graph convolutional transfer learning network (DAGCTLN) under a low-label ratio. Specifically, they constructed a novel DAGCTLN model consisting of a feature extractor, two label classifiers, and a discriminator, achieving the diagnosis of composite faults in the transfer domain and unseen faults in the source and target domains. Although sound signal classification has been widely applied in natural language processing and environmental sound processing, there are still technical bottlenecks in using sound signals for fault diagnosis in air compressor systems. This is primarily due to the complex and variable operating conditions of air compressors, as well as the presence of significant environmental noise.

To address these challenges, we propose an air compressor fault diagnosis model based on a low-rank matrix recovery algorithm. This model aims to mitigate the impact of environmental noise and complex operating conditions inherent in air compressors. An overview of the contributions of this paper is as follows:

1)The low-rank matrix recovery algorithm is utilized to effectively model the background of the Mel Frequency Cepstrum Coefficient (MFCC) spectrogram. By distinguishing foreground features from background noise, this approach helps in reducing interference and consequently lessens the computational burden on deep learning neural networks.

2)In the proposed method, the MobileNetV2 model is employed to extract features from the spectrogram images. Additionally, Principal Component Analysis (PCA) is applied to reduce the dimensionality of the extracted features,

Manuscript received May 11, 2024; revised September 20, 2024.

This work was supported by the Science and Technology Project of Jilin Province under Grant 20240101354JC.

Tianming Yu is an associate professor of the School of Automation Engineering, Northeast Electric Power University, Jilin, Jilin 132012 China. (e-mail: 20192928@neepu.edu.cn).

Cheng Long is a postgraduate student of the School of Information and Control Engineering, Jilin Institute of Chemical Technology, Jilin, Jilin 100190 China. (e-mail: chenglong_1023@163.com).

Guoliang Feng is a professor of the School of Automation Engineering, Northeast Electric Power University, Jilin, Jilin 132012 China. (e-mail: fengguoliang@neepu.edu.cn).

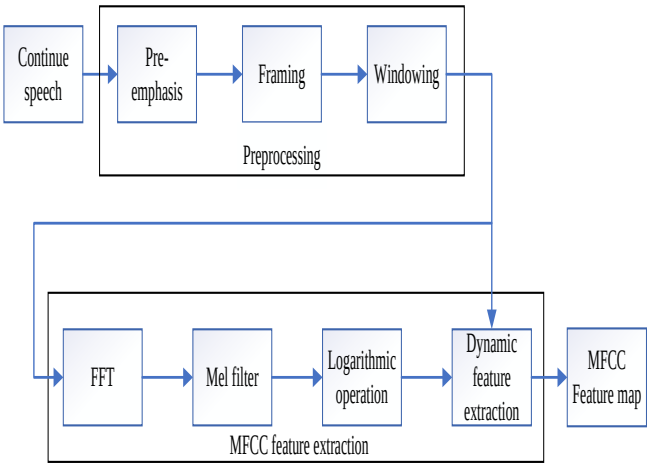

Fig. 1. MFCC feature extraction flowchart

facilitating efficient processing. Subsequently, k-means clustering analysis is conducted on the fault features of the air compressor to categorize and identify fault patterns. This integrated approach not only addresses the challenges posed by environmental noise and variable operating conditions but also enhances the efficiency and accuracy of fault diagnosis in air compressors. By leveraging techniques such as low-rank matrix recovery, feature extraction using MobileNetV2, dimensionality reduction with PCA, and fault pattern analysis via k-means clustering, the model offers a promising solution to the technical bottlenecks encountered in fault diagnosis based on sound signals in the domain of air compressor systems.

II. THEORETICAL BACKGROUND

A. Mel frequency cepstrum coefficient

The Mel Frequency Cepstral Coefficient (MFCC) [15] is a widely used feature extraction algorithm in speech and audio signal processing. It addresses the nonlinear relationship between perceived pitch and frequency in the human auditory system. To achieve this, the algorithm first converts the input signal into a frequency power spectrum and then applies cepstral analysis to derive features suitable for auditory perception. As a result, obtaining an optimal parametric representation of noisy signals becomes crucial for enhanced fault detection [16].

The MEL scale, upon which MFCC is based, is a nonlinear frequency scale that reflects the human ear's perception of isometric pitch changes. In this scale, f represents the input sound frequency, and the transformation relationship between sound frequency and Mel frequency can be expressed as follows [17]:

$$\mathbf{Mel}(f) = 2591\mathbf{lg}(1 + \frac{\mathbf{f}}{700}) \tag{1}$$

Given the input sound frequency f , MFCC consists of six calculation steps: preprocessing (pre-emphasis, framing, windowing), fast Fourier transform (FFT), constructing Mel filter banks, logarithmic operation, discrete cosine transform (DCT), and dynamic feature extraction. The MFCC feature extraction process is illustrated in figure 1.

B. Low rank matrix recovery

Low-rank matrix recovery, also known as Robust PCA [18], [19] or sparse and low-rank matrix factorization [20], is a technique used to decompose a given matrix into low-rank and sparse components.

Principal Component Analysis (PCA) is a fundamental method in data analysis that aims to find and construct low-dimensional feature spaces from high-dimensional data samples.

Consider a known observation data matrix M, which can be decomposed into a low-rank matrix L and a sparse matrix S, such that M = L + S. Here, L is of low rank, and S is sparse with potentially large non-zero elements. The goal is to recover L to obtain S.

To solve for L, we seek the minimum rank of L that can reconstruct the observed data, while ensuring that the error term is sparse. This can be formulated as the following optimization problem:

$$\begin{aligned} &\min_{L,S} \operatorname{rank}(L) + \delta\|S\|_0 \\ &\text{s.t.} \quad L + S = M \end{aligned} \tag{2}$$

Among them, $rank(L)$ represents the rank of matrix L, and $|\bullet|_0$ represents the norm of L_0.

III. FAULT DIAGNOSIS METHODS

A. Overall structure

When an air compressor operates, the high noise environment and the absence of labeled datasets often pose significant challenges for fault diagnosis. To address this issue, a MFCC-based fault diagnosis method employing low-rank background modeling is proposed, with faults categorized through unsupervised k-means clustering. The overall method is depicted in figure 2, and the specific steps are as follows:

1) Preprocess the noise data from the air compressor and extract its MFCC features.

2) Utilize low-rank background modeling to segregate background and foreground MFCC features, extracting the foreground MFCC features.

3) Classify the MFCC foreground features into abnormal and normal categories. Train the abnormal MFCC foreground features using the VGG16 model.

4) Identify and predict the foreground features of the MFCC test set. Extract the identified abnormal category images for subsequent k-means clustering analysis.

5) Employ the MobileNetV2 model to extract features from images. Reduce the dimensionality of the extracted features using PCA (Principal Component Analysis), and perform k-means clustering analysis on the predicted image features.

This method integrates MFCC feature extraction, low-rank background modeling, and unsupervised clustering to enable robust fault diagnosis in air compressors amidst challenging environmental conditions.

B. MFCC foreground feature extraction based on low-rank matrix recovery using IALM

During the process of sample classification, the presence of significant noise can significantly undermine the classifier's

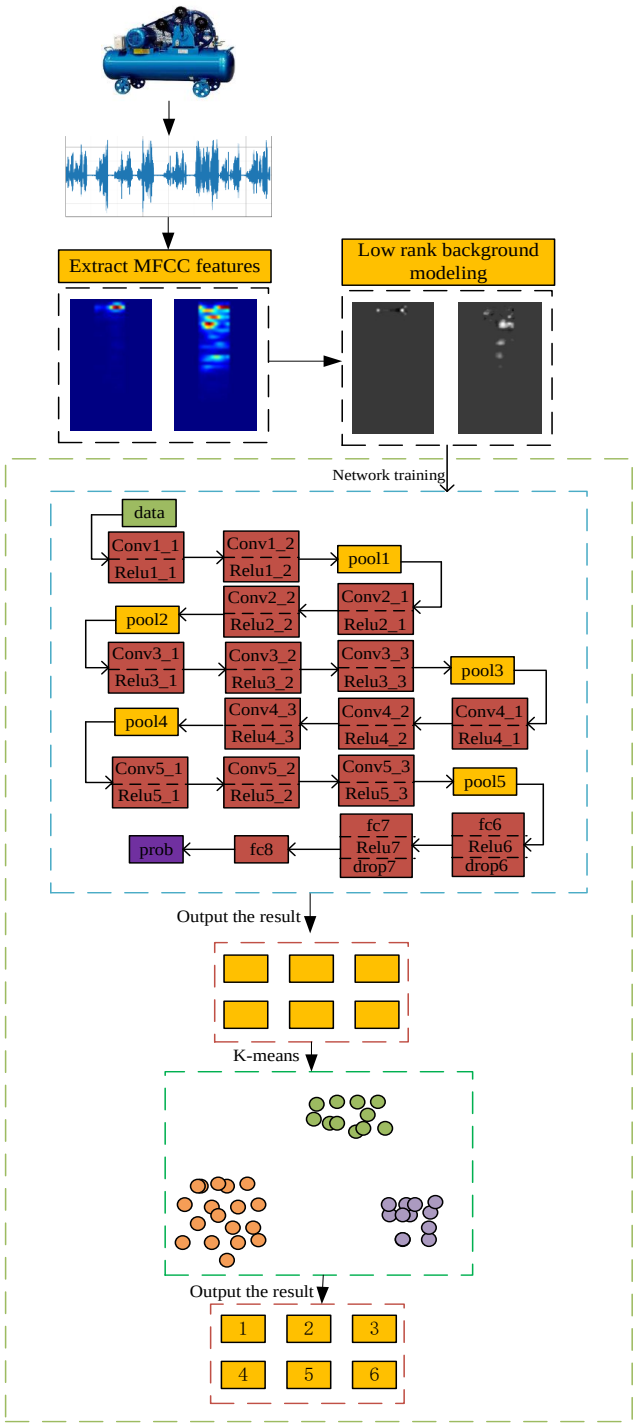

Fig. 2. Overall flowchart

prediction accuracy and increase computational overhead. To enhance denoising efficacy, improve classification accuracy, and reduce computation time, this paper introduces a denoising method based on low-rank matrix recovery using the IALM algorithm [21], [22] outlined in Algorithm 1:

Figure 3 depicts the MFCC characteristic spectrum of the air compressor and the foreground characteristic map after background modeling. MFCC features are extracted from the air compressor's audio noise dataset in WAV format, resulting in the MFCC feature spectrum. Subsequently, background modeling is performed to extract foreground features. As illustrated in figure 3, background modeling identifies

Algorithm 1 IALM algorithm for low rank matrix recovery

Initialize $Y_0, L_0 = 0, \mu_0, K = 0$,
While Non convergence do
$S_{k+1} = D_{\lambda\mu k^{-1}}\left[M - L_k + {\mu_k}^{-1} Y_k\right]$,
$(U, Sigma, V) = svd\left(M - S_{k+1} + {\mu_k}^{-1} Y_k\right)$,
$L_{k+1} = U A_{\mu k^{-1}}\left[Sigma\right] V^T$,
$Y_{k+1} = Y_k + \mu_k\left(M - L_{k+1} - S_{k+1}\right)$,
$Update\ \mu_k$,
$k = k + 1$
Output recovery matrix, optimal solution (L, S).

key features in the MFCC spectrum, thereby generating new features.

C. GFCC feature extraction

GFCC features can be categorized into time-domain and frequency-domain features. The concept of time-domain GFCC features was initially introduced in document [23]. The Gammatone filter is a filter bank based on the human cochlear auditory model, which effectively simulates the frequency division characteristics of the basilar membrane. Its time-domain expression is as follows:

$$g_i(t) = At^{n-1} e^{-2\pi b_i t} \cos\left(2\pi f_i + \varphi_i\right) v(t), \quad t \geq 0, 1 \leq i \leq N \tag{3}$$

GFCC feature parameter extraction follows a process similar to MFCC. After preprocessing, where the audio signal is converted to the frequency domain, the energy spectrum undergoes logarithmic compression via the gammatone filter bank. Subsequently, the discrete cosine transform is applied to obtain the GFCC feature parameters. Figure 4 illustrates the characteristics of the GFCC spectrum of the air compressor.

D. Deep learning noise classification based on vgg16 architecture

The VGG16 model effectively extracts fine-grained features within its receptive field by utilizing numerous 3x3 convolutional kernels. Each 3x3 convolution kernel can perceive information from the smallest receptive field in all directions - upper, lower, left, right, and center. The combination of two 3x3 convolution kernels results in a receptive field equivalent to a 5x5 convolution kernel, while three such convolutions create a receptive field equivalent to a 7x7 convolution kernel [24]. The model comprises 16 weight layers, including 13 convolution layers and 3 fully connected layers [25]. The convolution layers extract hierarchical features from input abnormal and normal foreground images, while the fully connected layers make final classification decisions.

Data preprocessing is crucial for enhancing the model's generalization ability. Images are randomly horizontally flipped for augmentation and normalized to ensure consistent input features. The preprocessed images are batch inputted into the VGG16 model. Stochastic Gradient Descent (SGD) with momentum is employed to optimize the model. The cross-entropy loss function calculates the discrepancy between predicted and actual tags. The training process occurs over multiple epochs, with model parameters continuously

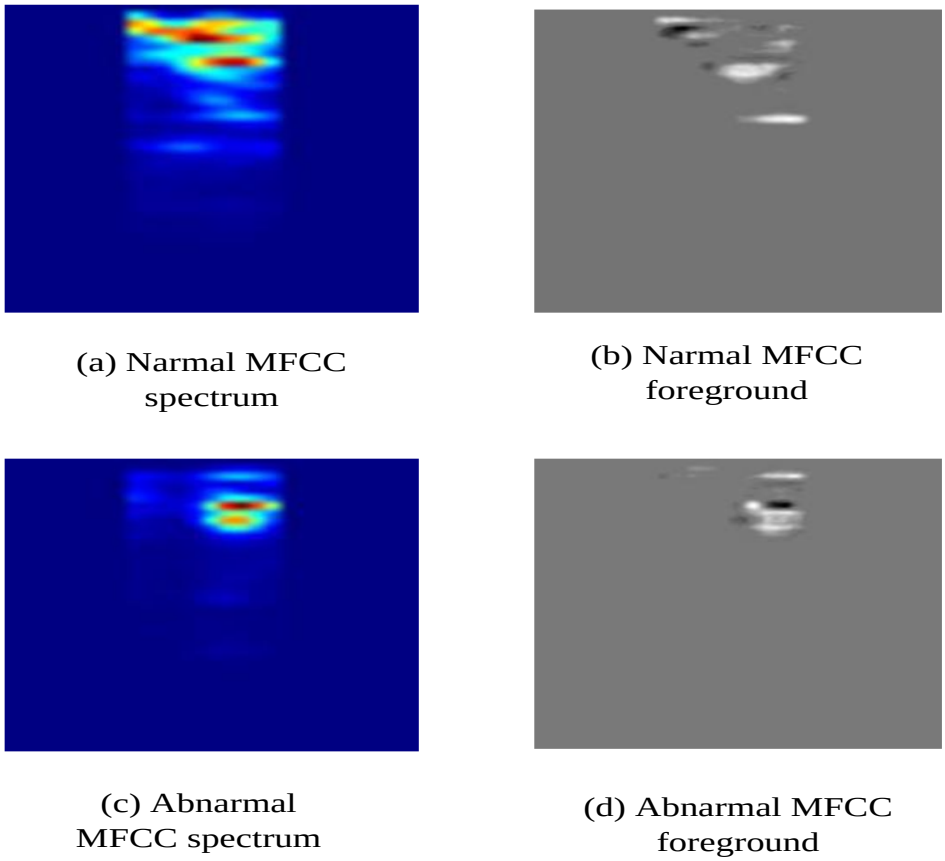

Fig. 3. MFCC spectrum and foreground

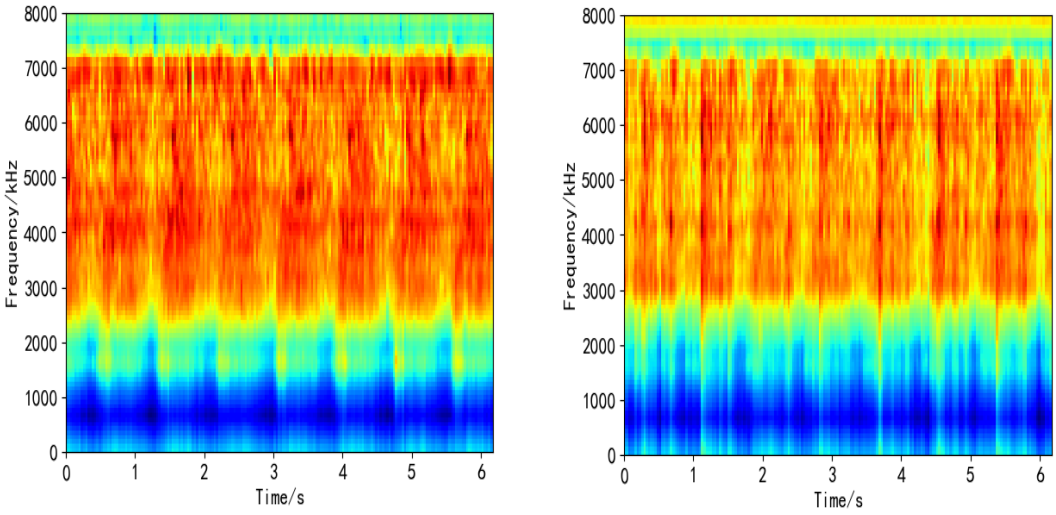

Fig. 4. GFCC spectrum

updated to enhance performance. Evaluation on an independent test set is conducted after each epoch, with accuracy serving as a metric to gauge the model's ability to correctly classify images as noisy or clear.

E. Image clustering based on K-means algorithm

In the absence of labeled training data, unsupervised clustering, particularly the k-means algorithm, has proven to be a potent method for grouping similar images based on extracted features. The MobileNetV2 model is employed to extract features from the images. To enhance efficiency, Principal Component Analysis (PCA) is utilized to reduce the dimensionality of the feature vector to two components. The reduced-dimension feature vector is then inputted into the K-means clustering algorithm.

The k-means algorithm iteratively partitions the image into K clusters, with the value of K determined by evaluation indices such as the CH index and SC index. Continuously updating the position of the cluster centers based on the

TABLE I
DATASET 1 BASIC INFORMATION

operational state	serial number	quantities(training set/test set)
normal	Normal-GFCC	135(45)
abnormal	abnormal-GFCC	945(315)

TABLE II
DATASET 2 BASIC INFORMATION

operational state	serial number	quantities(training set/test set)
normal	MFCC- foreground	135(45)
abnormal	MFCC- foreground	945(315)

similarity between data objects and cluster centers, the algorithm aims to minimize the sum of squared error (SSE) of the clusters. When SSE no longer changes or the objective function converges, the clustering process concludes, and the final clustering result is obtained.

As illustrated in figure 5, the original dataset comprises three clusters. The k-means algorithm is applied to cluster the dataset, and the final clustering result is achieved after two iterations of the dataset.

IV. EXPERIMENTAL RESULTS AND ANALYSIS

A. Data preprocessing

This dataset comprises data collected through acoustic recordings from a single-stage reciprocating air compressor, with a sampling frequency of 16 kHz. It consists of 1,800 audio recordings, encompassing both normal and seven fault states. The seven fault states include: inlet valve leakage (LIV) fault, outlet valve leakage (LOV) fault, check valve (NRV) fault, piston ring fault, flywheel fault, rider belt fault, and bearing fault, with each fault state containing 225 data samples. These fault states are evenly categorized into abnormal (Abnormal) types, while the normal state is classified as Normal.

Dataset 1 contains GFCC spectrograms extracted from audio data of the Abnormal class. Dataset 2 includes MFCC foreground images obtained from audio data of the Abnormal class after MFCC feature extraction and low-rank background modeling.

Both dataset 1 and dataset 2 are segmented into training, testing, and validation sets in a ratio of 0.6:0.2:0.2. Table 1 provides fundamental details regarding the air compressor noise dataset 1, while table 2 outlines the basic information concerning dataset 2.

B. Experimental results

In accordance with the structural framework of the air compressor fault diagnosis method, testing was conducted. Various networks were trained using single GFCC spectrum inputs and MFCC foreground noise maps after low-rank background modeling. Subsequently, the effectiveness of the low-rank background modeling method for air compressor fault detection was evaluated using unsupervised k-means algorithm clustering analysis.

1) Comparative analysis of single GFCC feature and MFCC foreground feature recognition results: The network models constructed using VGG16, VGG19, Resnet, Resnet34 and Resnet50 were compared and trained. These 5 models are evaluated based on accuracy, recall, and F1 score. Table 3 provides a detailed comparison of the performance of different neural network models on two different datasets. Comparative indicators include accuracy, F1 score, recall rate, and calculation time. The results showed that the VGG19 model achieved the highest accuracy of 100% on Data 1, followed closely by the VGG16 and Resnet models with accuracies of 99.70% and 99.36%, respectively. The VGG16 model also performs well in terms of F1 score and recall, both reaching full marks. However, the computation time of VGG16 is significantly higher at 8372 seconds, while the Resnet model shows faster processing times, with Resnet at 473 seconds and Resnet34 at 870 seconds.

On data 2, VGG16 once again performed excellently, with an accuracy of 91.40%, an F1 score of 0.90, and a recall rate of 0.92. It is worth noting that, the time required to train the model on dataset 1 is approximately 4.85 times and 2.13 times that of dataset 2. The reason for this difference is that foreground features are extracted through background modeling, and eliminating the background can reduce the image area that needs to be processed by the model, thereby reducing computational and storage costs.

2) Comparative analysis of single GFCC feature and background modeling foreground feature clustering results: In order to realize the clustering of air compressor faults and verify the effectiveness of the proposed algorithm, a total of 1575 groups of data in 7 abnormal states of air compressor are used in this paper. Mobilenetv2 model is used to extract features from single GFCC spectrum and MFCC foreground, and PCA (principal component analysis) is used to reduce the dimension of the extracted features, and cluster the features of the input images. Considering the ch index and SC index, the number of clusters is obtained, and the number of clusters is determined as 7. Table 4 shows the partial results of the two evaluation indicators in the GFCC spectrum diagram, and table 5 shows the partial results of the two evaluation indicators in the MFCC prospect diagram.

Table 4 and table 5 demonstrate that the Cluster Calinski Harabasz (CH) index and Silhouette Coefficient (SC) of the Mel Frequency Cepstrum Coefficient (MFCC) foreground map, obtained through low-rank background modeling, generally surpass those of the Single Gamma Tone Frequency Cepstrum Coefficient (GFCC) spectrum map. Furthermore, there is a significant reduction in processing time. Notably, figure 6(a) illustrates that during the clustering of MFCC foreground mapping, as the clustering parameter k approaches the inherent data categories, the CH index consistently rises. Conversely, when k surpasses the real data categories, the CH index experiences sudden fluctuations, displaying a notable inflection point in the line chart. Analyzing these significant inflection points on the CH index curve derived from the MFCC prospect map aids in identifying the data categories.

In contrast, the clustering process of the single GFCC spectrum witnesses significant fluctuations in both SC and CH indices, rendering the determination of the optimal clustering parameter K challenging based solely on these metrics. Consequently, precise classification of data categories through evaluation indices becomes problematic.

To further validate the effectiveness of the clustering method, data experiments with k=4 , and k=5 for the cluster-

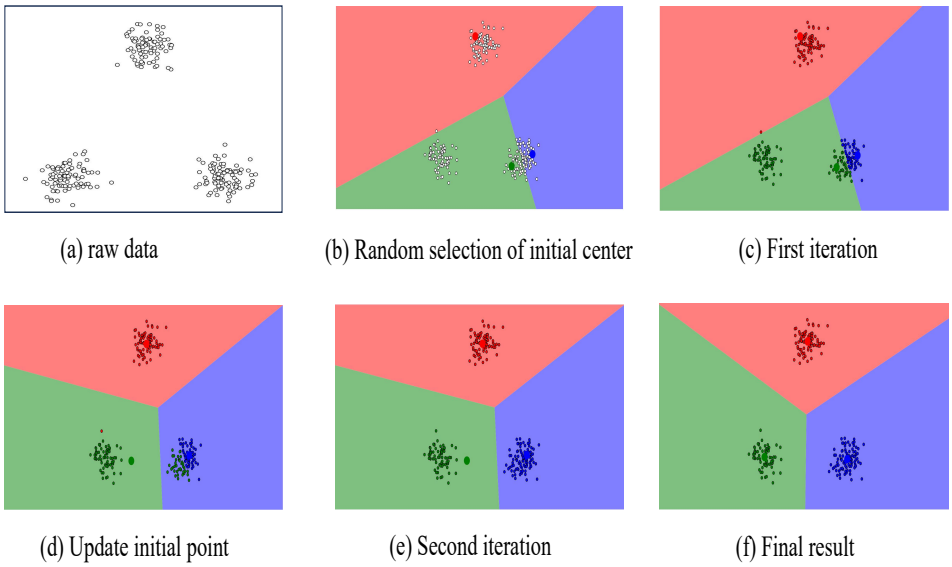

Fig. 5. K-means clustering flow chart

TABLE III
COMPARISON OF GFCC SPECTRUM AND MFCC FOREGROUND MODEL TRAINING RESULT

Neural Network Model	Data 1 Accuracy	F1-score	Recall	Time (s)	Data 2 Accuracy	F1-score	Recall	Tim (s)
VGG16	99.70%	1.00	1.00	8372	91.40%	0.90	0.92	1727
VGG19	100%	1.00	0.99	4076	95.90%	0.91	0.93	1916
Resnet	99.36%	0.98	0.98	473	85.94%	0.82	0.80	144
Resnet34	99.40%	0.99	1.00	870	94.10%	0.89	0.87	765
Resnet50	97.13%	0.95	0.92	2850	94.88%	0.91	0.93	826

TABLE IV
COMPARISON OF CLUSTERING INDICES FOR DIFFERENT K-VALUES OF GFCC SPECTRUM.

K	2	3	4	5	6	7	8
CH	1513	1621	1329	1681	2075	1464	1504
SC	0.587	0.399	0.385	0.375	0.347	0.377	0.358
Time(s)	34	30	30	31	42	39	35

TABLE V
COMPARISON OF CLUSTERING INDICES FOR DIFFERENT K-VALUES OF MFCC FOREGROUND MAP

K	2	3	4	5	6	7	8
CH	2708	3275	3750	4578	4969	5683	4992
SC	0.572	0.531	0.507	0.515	0.503	0.508	0.443
Time(s)	22	25	26	29	30	31	36

ing algorithm of air compressor faults were conducted. The experimental results are illustrated in figure 6(b).

Combined with the above experiments and analysis, it can be concluded that the MFCC foreground map after low rank background modeling can get more optimized results in terms of clustering effect, and can be effectively applied to the clustering of air compressor fault data to meet the needs of practical application.

V. CONCLUSIONS

The deep learning neural network, employing the IALM low rank matrix recovery algorithm as proposed in this paper, demonstrates superior performance in both classification and k-means clustering when compared to traditional single GFCC spectrum methods. Notably, the MFCC foreground map generated through the IALM low rank matrix recovery algorithm exhibits greater stability, facilitating more effective training of deep learning models and yielding improved clustering results for air compressor data.

By leveraging the proposed algorithm alongside air compressor data, unlabeled faults within the air compressor system can be accurately clustered into seven distinct categories. This comprehensive approach offers enhanced recognition and clustering capabilities for fault detection within air compressor systems, thereby providing a more precise and thorough fault detection framework.

REFERENCES

[1] S. Aravinth and V. Sugumaran, "Air compressor fault diagnosis through statistical feature extraction and random forest classifier," *Progress in Industrial Ecology, an International Journal*, vol. 12, no. 1-2, pp. 192–205, 2018.

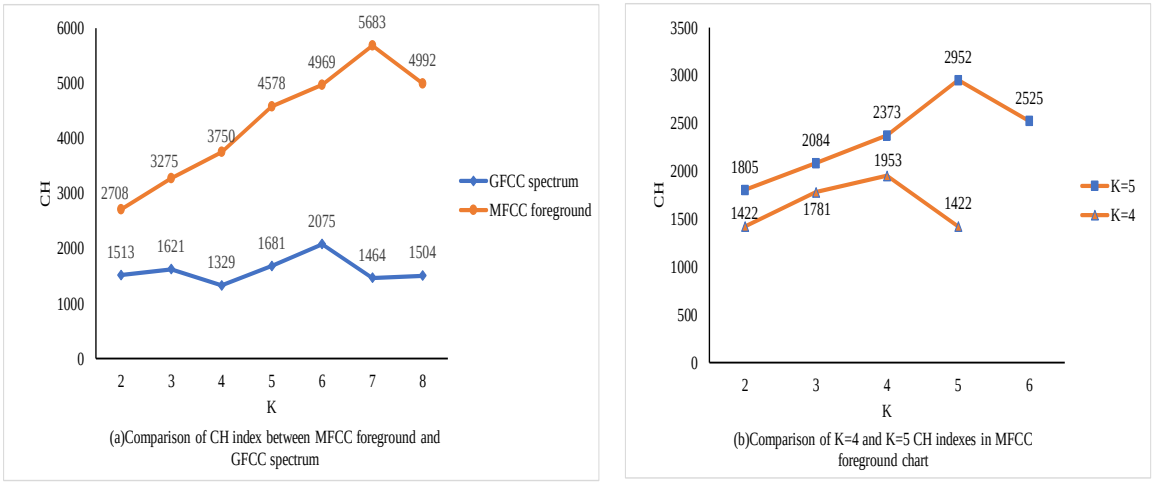

Fig. 6. Comparison of K-means clustering CH index line graph

[2] K. He, X. Zhang, S. Ren, and J. Sun, "Deep residual learning for image recognition," in *Proceedings of the IEEE conference on computer vision and pattern recognition*, 2016, pp. 770–778.

[3] R. Collobert and J. Weston, "A unified architecture for natural language processing: Deep neural networks with multitask learning," in *Proceedings of the 25th international conference on Machine learning*, 2008, pp. 160–167.

[4] Z. Wang, J. Wang, and Y. Sun, "Review of spectrum analysis in fault diagnosis for mechanical equipment," *Engineering Research Express*, vol. 5, no. 4, p. 042001, 2023.

[5] D. Jiang and Z. Wang, "Research on mechanical equipment fault diagnosis method based on deep learning and information fusion," *Sensors*, vol. 23, no. 15, p. 6999, 2023.

[6] K. Chen, Z. Liu, Q. Liu, Q. Ai, and L. Ma, "Eeg-based mental fatigue detection using linear prediction cepstral coefficients and riemann spatial covariance matrix," *Journal of Neural Engineering*, vol. 19, no. 6, p. 066021, 2022.

[7] J. Yuan, L. Li, H. Shao, M. Han, and H. Huang, "Material recognition for fault diagnosis in machine tools using improved mel frequency cepstral coefficients," *Journal of Manufacturing Processes*, vol. 98, pp. 67–79, 2023.

[8] B. K. Swain, M. Z. Khan, C. L. Chowdhary, and A. Alsaeedi, "Src: Superior robustness of covid-19 detection from noisy cough data using gfcc." *Computer Systems Science & Engineering*, vol. 46, no. 2, 2023.

[9] F. Yang and X. Li, "Research on substation monitoring and fault diagnosis based on distributed computing and artificial neural network," *Parallel Processing Letters*, vol. 33, no. 03, p. 2340004, 2023.

[10] F. Yao, Z. Chen, X. Liu, and M. Zhang, "Weak thruster fault detection for auv based on bayesian network and hidden markov model," *Proceedings of the Institution of Mechanical Engineers, Part M: Journal of Engineering for the Maritime Environment*, vol. 237, no. 2, pp. 478–486, 2023.

[11] A. Mathur, P. Kumar, and S. Harsha, "Ranked feature-based data-driven bearing fault diagnosis using support vector machine and artificial neural network," *Proceedings of the Institution of Mechanical Engineers, Part I: Journal of Systems and Control Engineering*, vol. 237, no. 9, pp. 1602–1619, 2023.

[12] D.-T. Hoang and H.-J. Kang, "A survey on deep learning based bearing fault diagnosis," *Neurocomputing*, vol. 335, pp. 327–335, 2019.

[13] O. Janssens, V. Slavkovikj, B. Vervisch, K. Stockman, M. Loccufier, S. Verstockt, R. Van de Walle, and S. Van Hoecke, "Convolutional neural network based fault detection for rotating machinery," *Journal of Sound and Vibration*, vol. 377, pp. 331–345, 2016.

[14] S. Yuanhao, M. Liang, X. Tongle, K. Xiaojia, L. Xiaosheng, and L. Yunfeng, "Wind turbine gearbox fault diagnosis method for optimized wgan with unbalanced data sets," *Acta Energiae Solaris Sinica*, vol. 43, no. 11, pp. 148–155, 2022.

[15] V. Chandrasekaran, S. Sanghavi, P. A. Parrilo, and A. S. Willsky, "Rank-sparsity incoherence for matrix decomposition," *SIAM Journal on Optimization*, vol. 21, no. 2, pp. 572–596, 2011.

[16] C.-C. Chang, "A library for support vector machines," *http://www. csie. ntu. edu. tw/˜ cjlin/libsvm*, 2001.

[17] F. Zheng, G. Zhang, and Z. Song, "Comparison of different implementations of mfcc," *Journal of Computer science and Technology*, vol. 16, pp. 582–589, 2001.

[18] J. Wright, A. Ganesh, S. Rao, Y. Peng, and Y. Ma, "Robust principal component analysis: Exact recovery of corrupted low-rank matrices via convex optimization," *Advances in neural information processing systems*, vol. 22, 2009.

[19] E. J. Candès, X. Li, Y. Ma, and J. Wright, "Robust principal component analysis?" *Journal of the ACM (JACM)*, vol. 58, no. 3, pp. 1–37, 2011.

[20] B. Y. Wang and X. G. Wang, "Research on background modeling based on low-rank matrix recovery," *Applied Mechanics and Materials*, vol. 635, pp. 1056–1059, 2014.

[21] Z. Lin, M. Chen, and Y. Ma, "The augmented lagrange multiplier method for exact recovery of corrupted low-rank matrices," *arXiv preprint arXiv:1009.5055*, 2010.

[22] M. Chen, Z. Lin, and X. Shen, "Algorithms and implementations of matrix reconstruction," *University of Chinese Academy of Sciences, Beijing*, 2010.

[23] J. Qi, D. Wang, Y. Jiang, and R. Liu, "Auditory features based on gammatone filters for robust speech recognition," in *2013 IEEE International Symposium on Circuits and Systems (ISCAS)*. IEEE, 2013, pp. 305–308.

[24] C. Shu and X. Hu, "Improved image style transfer based on vgg-16 convolutional neural network model," in *Journal of Physics: Conference Series*, vol. 2424, no. 1. IOP Publishing, 2023, p. 012021.

[25] J. Qiu, X. Lu, X. Wang, and X. Hu, "Research on rice disease identification model based on migration learning in vgg network," *IOP Conference Series: Earth and Environmental Science*, vol. 680, no. 1, p. 012087 (10pp), 2021.